JOURNAL OF AIRCRAFT
Vol. 35, No. 1, January–February 1998

Motion Analysis of Two Cable-Connected Bodies in Atmospheric Free-Fall

Shlomo Djerassi* and Zvi Viderman†
RAFAEL, Ministry of Defense, Haifa 31021, Israel

Occasionally, missions of missiles are aborted shortly after launch. It is common practice in such events to activate self-destruct mechanisms that cause the explosion of the missiles and the dispersion of debris over large areas. This work presents an alternative approach to mission termination. Given a mission abortion signal, the missile is separated by means such as explosive bolts into two parts, connected to one another by a cable. A 1000-kg missile is considered, separated into a 200-kg, aerodynamically unstable part and an 800-kg, aerodynamically stable part. It is shown that if the altitude of the separation zone is 2000–10,000 m, the resulting motion causes the missile parts to hit the ground after traversing a horizontal distance, which essentially depends on the missile horizontal speed at the time of separation if the missile was in the subsonic range, and that, within limits, this result depends weakly on the exact length of the cable and on the locations of the cable attachment points. Here the idea is presented together with an analysis supporting the indicated results and evaluating the impulses exerted during motion on the missile parts by means of the cable.

Introduction

THE Ariane Failure Report[1] recounts the chain of events leading to the disintegration of the Ariane V501 launcher. The launcher self-destruct system had been triggered by the separation of the booster from the main engine. The ensuing explosion, occurring at an altitude of approximately 4000 m, led to launcher disintegration and to the formation of debris scattered over an area of approximately 12 km^2. Recovery of the debris proved to be difficult. Similar events are reported[2] in connection with the failure of the Theater High Altitude Area Defence (THAAD) antimissile interceptor.

At times, it may be found beneficial to refrain from the use of explosives in self-destruct mechanisms, to prevent additional damage and to facilitate debris recovery. In such events, the following idea may be useful. At the time of mission abortion, designated T, explosive bolts are activated, separating the missile into two parts, A and B, as shown in Fig. 1. These parts remain connected to one another by means of a cable of length L, attached to points $\bar{A}$ and $\bar{B}$ of A and B, respectively. The cable is initially, i.e., at time T, loose, and the set of forces exerted on A and B (mainly aerodynamic and gravitational forces) cause the distance between $\bar{A}$ and $\bar{B}$ to increase. When this distance becomes L, $\bar{A}$ and $\bar{B}$ exert impulses on one another through the cable, which becomes instantaneously taut. A tumbling motion of both A and B is thus initiated. The distance between points $\bar{A}$ and $\bar{B}$ changes erratically, and the cable becomes alternately loose and taut. Consequently, A and B rapidly lose their horizontal velocity component, ultimately hitting the ground at a predictable horizontal distance from the separation zone. For example, suppose that A and B are composed of 0.5-m-diam cylinders weighing 200 and 800 kg, respectively, the cable is 1 m long, the missile moves horizontally with a speed of 200 m/s, and the altitude of the separation zone is 8000 m. If $T = 0$, then the path traversed by the mass center of B is shown by the solid line in Fig. 2. The intermittent line indicates the path traversed by the mass center of B if, with the same conditions at $T = 0$, B moves independently from A.

Motions of two bodies connected by means of a cable have been the subject of numerous investigations in connection with space,[3,4] airborne,[5,6] sea,[7,8] and land[9,10] applications. Typically, space, airborne, and sea applications involve long cables, i.e., as compared to the size of the bodies that are connected. Hence, the inertial properties of the cable, in addition to those of the bodies involved, are accounted for. By way of contrast, inertial properties of cables in land applications are usually disregarded, because cables in such applications are typically short. This makes it possible to replace the cables by rods.[11,12] However, rods impose kinematical constraints, whereas cables do so only if in tension. Otherwise, the cable is loose and the bodies move independently of one another. In an ongoing motion of two cable-connected bodies, which is of interest here, a constrained motion (taut cable) and an unconstrained motion (loose cable) may occur alternately. Moreover, the unconstrained motion is accompanied by impacts occurring when the cable becomes instantaneously taut, or when the bodies collide with one another. The studies in Refs. 9 and 10 do not deal with these issues, as only situations in which the cable is in tension throughout the motion are discussed.

It is the purpose of this work to generate equations governing motions of the system shown in Fig. 1 in atmospheric free-fall and to develop an algorithm dealing with situations in which the cable becomes instantaneously or continuously taut; to apply the algorithm to the system shown in Fig. 1; and to obtain predictions of the indicated motions. Specifically, the trajectory of the mass center of B and impulses occurring during motion are investigated.

The governing equations are generated in the following section. Next, simulation results of interest are reported and discussed. Conclusions concerning the present approach to mission abortion close this work.

Analysis

As indicated, the model shown in Fig. 1 represents S, the system in question, which consists of rigid bodies A and B and of a cable C. Assuming that the cable is loose, and that, therefore, A and B move independently of one another, one can

Received May 18, 1997; revision received July 29, 1997; accepted for publication Aug. 7, 1997; presented as Paper 97-3492 at the AIAA Atmospheric Flight Mechanics Conference, New Orleans, LA, Aug. 11–13, 1997.

*Chief R & D Engineer, P.O. Box 2250.
†Project Manager, P.O. Box 2250.

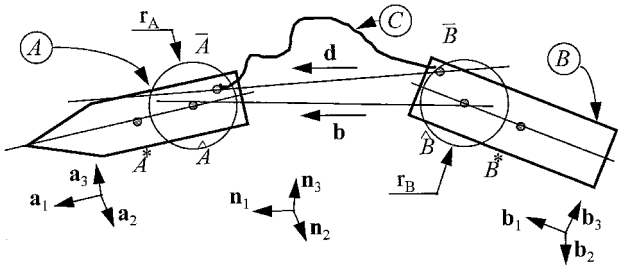

Fig. 1 System model after separation.

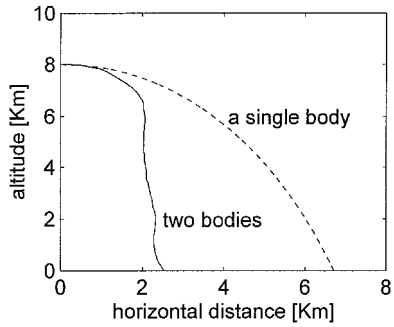

Fig. 2 Paths traversed by the mass center of *B*.

describe the motion of S in N, a Newtonian reference frame, as follows. Let $\boldsymbol{a}_i$ ($i = 1, 2, 3$), $\boldsymbol{b}_i$ ($i = 1, 2, 3$), and $\boldsymbol{n}_i$ ($i = 1, 2, 3$) be three sets of three dextral, mutually perpendicular unit vectors fixed in A, B, and N, respectively. Let $\boldsymbol{\omega}^A$ and $\boldsymbol{\omega}^B$ be the angular velocities of A and B in N, and $\boldsymbol{v}^{A^*}$ and $\boldsymbol{v}^{B^*}$ be the velocities of A^* and B^*, the mass centers of A and B, in N. Then 12 generalized speeds u_r ($r = 1, \ldots, 12$) can be defined, so that

$$\boldsymbol{\omega}^A = u_1\boldsymbol{a}_1 + u_2\boldsymbol{a}_2 + u_3\boldsymbol{a}_3 \tag{1}$$

$$\boldsymbol{v}^{A^*} = u_4\boldsymbol{n}_1 + u_5\boldsymbol{n}_2 + u_6\boldsymbol{n}_3 \tag{2}$$

$$\boldsymbol{\omega}^B = u_7\boldsymbol{b}_1 + u_8\boldsymbol{b}_2 + u_9\boldsymbol{b}_3 \tag{3}$$

$$\boldsymbol{v}^{B^*} = u_{10}\boldsymbol{n}_1 + u_{11}\boldsymbol{n}_2 + u_{12}\boldsymbol{n}_3 \tag{4}$$

Furthermore, assuming that $\boldsymbol{a}_i(1, 2, 3)$ and $\boldsymbol{b}_i(1, 2, 3)$ are parallel to the central principal axes of A and B, respectively, and denoting the associated moments of inertia of A and B I_1^A, I_2^A, I_3^A and I_1^B, I_2^B, I_3^B, and the masses of A and B m_A and m_B, respectively, one can generate the generalized inertia forces F_r^* ($r = 1, \ldots, 12$) for S straightforwardly (Ref. 13, Sec. 4.11). These are

$$\begin{aligned} F_1^* &= -I_1^A\dot{u}_1 - u_3u_2(I_3^A - I_2^A) \\ F_2^* &= -I_2^A\dot{u}_2 - u_1u_3(I_1^A - I_3^A) \\ F_3^* &= -I_3^A\dot{u}_3 - u_2u_1(I_2^A - I_1^A) \end{aligned} \tag{5}$$

$$F_4^* = -m_A\dot{u}_4, \qquad F_5^* = -m_A\dot{u}_5, \qquad F_6^* = -m_A\dot{u}_6 \tag{6}$$

$$\begin{aligned} F_7^* &= -I_1^B\dot{u}_7 - u_9u_8(I_3^B - I_2^B) \\ F_8^* &= -I_2^B\dot{u}_8 - u_7u_9(I_1^B - I_3^B) \\ F_9^* &= -I_3^B\dot{u}_9 - u_8u_7(I_2^B - I_1^B) \end{aligned} \tag{7}$$

$$F_{10}^* = -m_B\dot{u}_{10}, \qquad F_{11}^* = -m_B\dot{u}_{11}, \qquad F_{12}^* = -m_B\dot{u}_{12} \tag{8}$$

Now A and B are subject to aerodynamical forces and couples and to gravitational forces. The aerodynamical forces and couples can be written in terms of two angles, α and β, the former being the angle of attack, defined, in connection with A, as

$$\alpha \triangleq \cos^{-1}[v_1/(v_1^2 + v_2^2 + v_3^2)^{1/2}] \tag{9}$$

where, with no-wind conditions

$$v_i \triangleq \boldsymbol{v}^{A^*}\cdot\boldsymbol{a}_i \qquad i = 1, 2, 3$$

This definition allows α to take on values between zero and π, as might be the case if A undergoes tumbling. Next β is defined as the angle between the projection of $\boldsymbol{v}^{A^*}$ on a plane parallel to $\boldsymbol{a}_2$ and $\boldsymbol{a}_3$, say, the plane containing A^*, and a vector parallel to $\boldsymbol{a}_2$ and lying in the indicated plane; that is,

$$\begin{aligned} \beta \triangleq\ & (1 + v_3/|v_3|)\cos^{-1}[v_2/(v_2^2 + v_3^2)^{1/2}]/2 \\ & + (1 - v_3/|v_3|)\{2\pi - \cos^{-1}[v_2/(v_2^2 + v_3^2)^{1/2}]\}/2 \end{aligned} \tag{10}$$

Thus, β may vary between zero and 2π. One can now define the following three dextral, mutually perpendicular unit vectors, namely:

$$\boldsymbol{a}_1' = \cos(\alpha)\boldsymbol{a}_1 + \sin(\alpha)\cos(\beta)\boldsymbol{a}_2 + \sin(\alpha)\sin(\beta)\boldsymbol{a}_3 \tag{11}$$

$$\begin{aligned} \boldsymbol{a}_2' = [&\sin(\alpha)\boldsymbol{a}_1 - \cos(\alpha)\cos(\beta)\boldsymbol{a}_2 \\ &- \cos(\alpha)\sin(\beta)\boldsymbol{a}_3]\mathrm{sgn}(\pi/2 - \alpha) \end{aligned} \tag{12}$$

$$\boldsymbol{a}_3' = [\sin(\beta)\boldsymbol{a}_2 - \cos(\beta)\boldsymbol{a}_3]\mathrm{sgn}(\pi/2 - \alpha) \tag{13}$$

The function $\mathrm{sgn}(\pi/2 - \alpha)$ is used to validate the following approximate expressions for the lift force $\boldsymbol{L}^{A^*}$ and the drag force $\boldsymbol{D}^{A^*}$, both exerted on A^*, and the pitch couple of torque $\boldsymbol{M}^A$ exerted on A for $0 \le \alpha \le \pi$, when written as follows:

$$\boldsymbol{L}^{A^*} = 1/2\rho(\boldsymbol{v}^{A^*})^2S_{\mathrm{ref}A}C_L\boldsymbol{a}_2' \tag{14}$$

$$\boldsymbol{D}^{A^*} = -1/2\rho(\boldsymbol{v}^{A^*})^2S_{\mathrm{ref}A}C_D\boldsymbol{a}_1' \tag{15}$$

$$\boldsymbol{M}^A = 1/2\rho(\boldsymbol{v}^{A^*})^2S_{\mathrm{ref}A}D_{\mathrm{ref}A}C_M\boldsymbol{a}_3' \tag{16}$$

Here, $S_{\mathrm{ref}A}$ and $D_{\mathrm{ref}A}$ are geometry-dependent constants, and C_L, C_D, and C_M are aerodynamic coefficients given for $\alpha \le \pi/2$ by

$$C_L = 1/2[A_A\sin(2\alpha) + B_A\cos(\alpha)\sin^2(\alpha)] \tag{17}$$

$$C_D = C_{AD_0} + C_A[1 - \cos(2\alpha)] \tag{18}$$

$$C_M = \Delta x_A[C_L\cos(\alpha) + C_D\sin(\alpha)] \tag{19}$$

where A_A, B_A, C_A, C_{AD_0}, and Δx_A are geometry-dependent constants. Expressions for $\pi/2 \le \alpha \le \pi$ are obtained from Eqs. (17–19), if α is replaced with $\pi - \alpha$.

Gravitational force can be expressed as

$$\boldsymbol{F}^{A^*} = -m_Ag\boldsymbol{n}_3 \tag{20}$$

where $\boldsymbol{n}_3$ is aligned with the local vertical and points upward, and g is the gravitational acceleration.

Expressions similar to those in Eqs. (9–20) can be written for B, so that the generalized active forces F_r ($r = 1, \ldots, 12$) (Ref. 13, Sec. 4.4) can be generated for S. Equations governing the motion of S can be formed if F_r ($r = 1, \ldots, 12$) are substituted, together with the generalized inertia forces given by Eqs. (5–8), in the following equations (Ref. 13, Sec. 6.1):

$$F_r + F_r^* = 0 \qquad r = 1, \ldots, 12 \tag{21}$$

Note that expressions (14–16) are based on approximations representing a certain missile configuration, that they disregard

aerodynamical interaction between the missile parts, and that no-wind conditions are assumed.

Three events may interfere with the continuous motion of S, as represented by Eqs. (21):

1) The cable may become instantaneously taut, inflicting an impact on A and B.

2) A and B may hit one another and, consequently, undergo an impact.

3) The cable may become continuously taut, imposing a constraint on the motion of S. The effects of these events on the motion of S are now considered in detail.

One may start with the first event, focusing attention on points $\bar{A}$ and $\bar{B}$, assumed to be connected to one another by means of an inextensible cable of length L. Suppose $\boldsymbol{v}^{\bar{A}}$ and $\boldsymbol{v}^{\bar{B}}$ are the velocities of $\bar{A}$ and $\bar{B}$ in N. In view of Eqs. (1–4), these can be written

$$\boldsymbol{v}^{\bar{A}} = \boldsymbol{v}^{A^*} + \boldsymbol{\omega}^A \times \boldsymbol{r}^{A^*\bar{A}}, \qquad \boldsymbol{v}^{\bar{B}} = \boldsymbol{v}^{B^*} + \boldsymbol{\omega}^B \times \boldsymbol{r}^{B^*\bar{B}} \tag{22}$$

where $\boldsymbol{r}^{A^*\bar{A}}$ and $\boldsymbol{r}^{B^*\bar{B}}$ are position vectors directed from A^* and B^* to $\bar{A}$ and $\bar{B}$, respectively. Accordingly, one can express $\boldsymbol{v}^{\bar{A}}$ and $\boldsymbol{v}^{\bar{B}}$ as

$$\boldsymbol{v}^{\bar{A}} = \sum_{r=1}^{12} \boldsymbol{v}_r^{\bar{A}} u_r, \qquad \boldsymbol{v}^{\bar{B}} = \sum_{r=1}^{12} \boldsymbol{v}_r^{\bar{B}} u_r \tag{23}$$

where $\boldsymbol{v}_r^{\bar{A}}$ and $\boldsymbol{v}_r^{\bar{B}}$ ($r = 1, \ldots, 12$), the coefficients of u_r ($r = 1, \ldots, 12$), are called partial velocities (Ref. 13, Sec. 2.14) and constitute configuration-dependent vectors, namely, vector functions of the generalized coordinates and time. Consequently, $\boldsymbol{v}^R$, the relative velocity of $\bar{A}$ and $\bar{B}$ given by

$$\boldsymbol{v}^R \triangleq \boldsymbol{v}^{\bar{A}} - \boldsymbol{v}^{\bar{B}} \tag{24}$$

can be expressed as

$$\boldsymbol{v}^R = \sum_{r=1}^{12} \boldsymbol{v}_r^R u_r \tag{25}$$

where $\boldsymbol{v}_r^R$ is defined as

$$\boldsymbol{v}_r^R \triangleq \boldsymbol{v}_r^{\bar{A}} - \boldsymbol{v}_r^{\bar{B}} \qquad r = 1, \ldots, 12 \tag{26}$$

Now suppose d is the distance from $\bar{A}$ to $\bar{B}$. It may occur that $d = L$ and $\dot{d} = |\boldsymbol{v}^R| > \dot{d}_0$, where $\dot{d}_0$ is an arbitrarily small quantity. Then the cable becomes taut, and A and B are subjected to impulsive forces through the cable. Moreover, if the associated impact, assumed to be elastic, starts at $t = t_1$ and terminates at $t = t_2$, so that $t_2 - t_1$ is infinitely small, one can write

$$\boldsymbol{v}^R \cdot \boldsymbol{d}\big|_{t_2} = -\boldsymbol{v}^R \cdot \boldsymbol{d}\big|_{t_1} \tag{27}$$

or

$$\boldsymbol{v}^R \cdot \boldsymbol{d}\big|_{t_2} - \boldsymbol{v}^R \cdot \boldsymbol{d}\big|_{t_1} = -2\boldsymbol{v}^R \cdot \boldsymbol{d}\big|_{t_1} \tag{28}$$

where $\boldsymbol{d}$ is a unit vector parallel to the line connecting $\bar{A}$ to $\bar{B}$ and pointing toward $\bar{A}$. If, in addition, both sides of Eq. (25) are dot multiplied with $\boldsymbol{d}$, that is,

$$\boldsymbol{v}^R \cdot \boldsymbol{d} = \sum_{r=1}^{12} \boldsymbol{v}_r^R \cdot \boldsymbol{d} u_r \tag{29}$$

and if Δu_r is defined as

$$\Delta u_r \triangleq u_r(t_2) - u_r(t_1) \qquad r = 1, \ldots, 12 \tag{30}$$

then, using Eqs. (28–30), one has

$$\sum_{r=1}^{12} \boldsymbol{v}_r^R \cdot \boldsymbol{d} \Delta u_r = -2\boldsymbol{v}^R \cdot \boldsymbol{d}\big|_{t_1} \tag{31}$$

Next Eqs. (21) are considered. It can be shown that if these are integrated from $t = t_1$ to $t = t_2$, the following equations result:

$$\sum_{s=1}^{12} m_{rs} \Delta u_s = -\int_{t_1}^{t_2} F_r \, dt \qquad r = 1, \ldots, 12 \tag{32}$$

where m_{rs} is the element in row r, column s of the mass matrix associated with Eqs. (21). Suppose that, during impact, point $\bar{A}$ exerts on point $\bar{B}$ a force $\boldsymbol{F}$ of magnitude F; that is, $\boldsymbol{F} = F\boldsymbol{d}$. Then, in accordance with the law of action and reaction, point $\bar{B}$ exerts on point $\bar{A}$ a force $-\boldsymbol{F}$; and if these are the only impulsive forces appearing in F_r ($r = 1, \ldots, 12$) between t_1 and t_2, then

$$\int_{t_1}^{t_2} F_r \, dt = \int_{t_1}^{t_2} [\boldsymbol{F} \cdot \boldsymbol{v}_r^{\bar{B}} + (-\boldsymbol{F}) \cdot \boldsymbol{v}_r^{\bar{A}}] \, dt = -\int_{t_1}^{t_2} \boldsymbol{F} \cdot \boldsymbol{v}_r^R \, dt$$
$$= -\int_{t_1}^{t_2} F \boldsymbol{v}_r^R \cdot \boldsymbol{d} \, dt = -\boldsymbol{v}_r^R \cdot \boldsymbol{d} \int_{t_1}^{t_2} F \, dt \tag{33}$$

where $\boldsymbol{v}_r^R \cdot \boldsymbol{d}$, being a configuration-dependent quantity (and, hence, remaining constant between t_1 and t_2), is removed from under the integral. If I is a quantity defined as

$$I \triangleq \int_{t_1}^{t_2} F \, dt \tag{34}$$

then, in connection with Eq. (33)

$$\int_{t_1}^{t_2} F_r \, dt = -I\boldsymbol{v}_r^R \cdot \boldsymbol{d} \qquad r = 1, \ldots, 12 \tag{35}$$

so that, in view of Eqs. (32)

$$\sum_{s=1}^{12} m_{rs} \Delta u_s = I\boldsymbol{v}_r^R \cdot \boldsymbol{d} \qquad r = 1, \ldots, 12 \tag{36}$$

Now, m_{rs} ($r, s = 1, \ldots, 12$) can be identified with the aid of Eqs. (5–8), namely,

$$\begin{aligned} m_{rr} &= -I_r^A (r = 1, 2, 3), \qquad m_{rr} = -m_A (r = 4, 5, 6) \\ m_{rr} &= -I_r^B (r = 7, 8, 9), \qquad m_{rr} = -m_B (r = 10, 11, 12) \end{aligned} \tag{37}$$

and, because $m_{rs} = 0$ if $r \neq s$, ($r, s = 1, \ldots, 12$), one has, with the aid of Eqs. (36)

$$\Delta u_r = I\boldsymbol{v}_r^R \cdot \boldsymbol{d}/m_{rr} \qquad r = 1, \ldots, 12 \tag{38}$$

Substituting Δu_r from Eq. (38) in Eq. (31), one obtains

$$I \sum_{r=1}^{12} (\boldsymbol{v}_r^R \cdot \boldsymbol{d})^2 / m_{rr} = -2\boldsymbol{v}^R \cdot \boldsymbol{d}\big|_{t_1} \tag{39}$$

an equation which, when solved for I, results in

$$I = -2\boldsymbol{v}^R \cdot \boldsymbol{d}\big|_{t_1} \Big/ \left[\sum_{r=1}^{12} (\boldsymbol{v}_r^R \cdot \boldsymbol{d})^2 / m_{rr} \right] \tag{40}$$

With I in hand, new values of generalized speeds resulting from the impact can be evaluated as follows:

$$u_r(t_2) = u_r(t_1) + I\boldsymbol{v}_r^R \cdot \boldsymbol{d}/m_{rr} \qquad r = 1, \ldots, 12 \qquad (41)$$

if use is made of Eqs. (38) and (30).

The second event concerns A and B hitting one another. An exact analytical description of this state of affairs might be extremely complex if A and B comprise complex bodies. To make the analytical treatment manageable, it is to be assumed here that the surfaces of A and B coming into contact during impact are spherical with radii r_A and r_B and centers located at point $\hat{A}$ and $\hat{B}$ of A and B, respectively (Fig. 1). Moreover, it is assumed that the coefficient of friction between the colliding surfaces is zero, which means that the tangential component of $\boldsymbol{v}^R$ remains intact during the impact (Ref. 13, Sec. 7.9). Now suppose b is the distance from $\hat{A}$ to $\hat{B}$, and $\boldsymbol{v}^R$ and $\boldsymbol{v}_r^R$ ($r = 1, \ldots, 12$) are redefined as $\boldsymbol{v}^R \triangleq \boldsymbol{v}^{\hat{A}} - \boldsymbol{v}^{\hat{B}}$ and $\boldsymbol{v}_r^R \triangleq \boldsymbol{v}_r^{\hat{A}} - \boldsymbol{v}_r^{\hat{B}}$ ($r = 1, \ldots, 12$), respectively. It may occur that $b = r_A + r_B$ and $\dot{b} = -|\boldsymbol{v}^R| < 0$. Then A and B undergo an impact assumed here to be elastic. The evaluation of the associated change in the generalized speeds proceeds as follows. Define a unit vector $\boldsymbol{b}$ parallel to the line connecting $\hat{A}$ and $\hat{B}$ and pointing toward $\hat{A}$. Then, during impact, $\hat{A}$ exerts on $\hat{B}$ a force of magnitude F through the surfaces of the indicated spheres, whereas $\hat{B}$ exerts on $\hat{A}$ a force $-\boldsymbol{F}$. Under these circumstances, Eq. (33) is replaced with

$$\int_{t_1}^{t_2} F_r \, \mathrm{d}t = \boldsymbol{v}_r^R \cdot \boldsymbol{b} \int_{t_1}^{t_2} F \, \mathrm{d}t \qquad (42)$$

where $\boldsymbol{v}_r^R \cdot \boldsymbol{b}$, being a configuration-dependent quantity, is removed from under the integral, and where now $\boldsymbol{F} = -F\boldsymbol{b}$. Equations similar to Eqs. (40) and (41) can be obtained, so that now

$$I = 2\boldsymbol{v}^R \cdot \boldsymbol{b}\,|_{t_1} \Big/ \left[\sum_{r=1}^{12} (\boldsymbol{v}_r^R \cdot \boldsymbol{b})^2 / m_{rr} \right] \qquad (43)$$

$$u_r(t_2) = u_r(t_1) - I\boldsymbol{v}_r^R \cdot \boldsymbol{b}/m_{rr} \qquad r = 1, \ldots, 12 \qquad (44)$$

Finally, the third event is considered. Accordingly, it may occur that $d = L$ and $0 < \dot{d} < \dot{d}_0$, an event that can be regarded as indicating transition to a motion with a taut cable. Such a motion is subject to the following constraint equation:

$$\boldsymbol{v}^R \cdot \boldsymbol{d} = 0 \qquad (45)$$

When written explicitly with the aid of Eqs. (1–4) and (24), Eq. (45) gives rise to a linear relation between $u_1, \ldots, u_{12}$, which, if solved for u_{12}, reads

$$u_{12} = \sum_{r=1}^{11} C_{12r} u_r \qquad (46)$$

where C_{12r} ($r = 1, \ldots, 11$) are given, in view of Eqs. (29) and (45), by

$$C_{12r} = -\boldsymbol{v}_r^R \cdot \boldsymbol{d}/\boldsymbol{v}_{12}^R \cdot \boldsymbol{d} \qquad r = 1, \ldots, 11 \qquad (47)$$

The equations governing the associated motion are (Ref. 13, Sec. 6.1)

$$F_r + F_r^* + C_{12r}(F_{12} + F_{12}^*) = 0 \qquad r = 1, \ldots, 11 \qquad (48)$$

Moreover, the cable might now become loose, a possibility that must be checked continuously, or, in the context of numerical integration, at each integration step. To do so, one may define R as $R \triangleq \boldsymbol{R} \cdot \boldsymbol{d}$, where $\boldsymbol{R}$ is the force exerted $\bar{A}$ on $\bar{B}$ through the cable when the cable is taut. The cable becomes loose when R first becomes negative, in which event Eqs. (21) resume their role as the governing equations. One must now determine R, a task made possible if the constraint in Eq. (46) is temporarily removed. Then u_{12} becomes an independent variable called auxiliary generalized speed (Ref. 13, Sec. 4.9). Equations (21) become valid again, except that now they include contributions from $\boldsymbol{R}$, namely, $\boldsymbol{v}_r^R \cdot \boldsymbol{R}$ ($r = 1, \ldots, 12$). The last of Eqs. (21) now reads

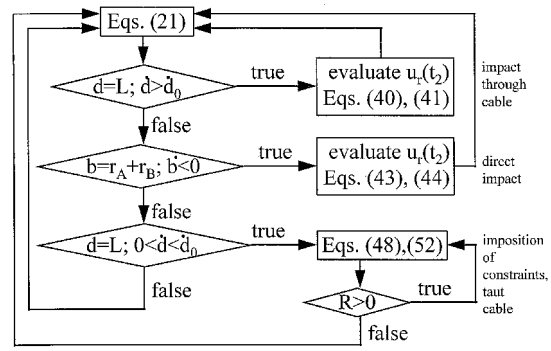

Fig. 3 Flow chart underlying the simulation code.

$$F_{12} + F_{12}^* + \boldsymbol{v}_{12}^R \cdot \boldsymbol{R} = 0 \qquad (49)$$

Moreover,

$$\boldsymbol{v}_{12}^R = \boldsymbol{v}_{12}^{\hat{A}} - \boldsymbol{v}_{12}^{\hat{B}} = -\boldsymbol{n}_3 \qquad (50)$$

a relation obtained with the aid of the last of Eqs. (26), and with Eqs. (22) and (1–4). One then has

$$F_{12} + F_{12}^* - R\boldsymbol{n}_3 \cdot \boldsymbol{d} = 0 \qquad (51)$$

Finally,

$$R = (F_{12} + F_{12}^*)/\boldsymbol{n}_3 \cdot \boldsymbol{d} \qquad (52)$$

One then has all of the ingredients required to construct a code simulating the motion of S. The flow chart in Fig. 3 summarizes the underlying algorithm. Accordingly, a simulation code had been constructed which, with the following parameter values, yields Fig. 2: $I_1^A = 6.25$, $I_2^A = I_3^A = 34$, $I_1^B = 25$, $I_2^B = I_3^B = 2000$ kg-m^2, $m_A = 200$, $m_B = 800$ kg, $A_A = 5$, $B_A = 10$, $C_A = 3$, $C_{AD_0} = 0.4$, $\Delta x_A = 1.6$, $A_B = 25$, $B_B = 50$, $C_B = 8$, $C_{BD_0} = 0.8$, $\Delta x_B = -0.5$, $S_{\mathrm{ref}A} = 0.2$ m^2, $D_{\mathrm{ref}A} = 0.5$ m, $S_{\mathrm{ref}B} = 0.2$ m^2, and $D_{\mathrm{ref}B} = 0.5$ m. It is also assumed that $\hat{A}$ and $\hat{B}$ are located at $-1.2\boldsymbol{a}_1$ and $1.2\boldsymbol{b}_1$ m relative to A^* and B^*, respectively, that $r_A = r_B = 0.79$ m, and that $\dot{d}_0 = 1$ m/s. Finally, the air density ρ is taken to be the following function of h, the altitude of B^*: $\rho = 0.00348368P/T$ kg-m^3, where $T = 288.16 - 0.0065h$, $P = 101325\,(T/288.16)^{5.256122}$.

Although the behavior of the two connected bodies seems erratic, Fig. 2 shows that the bodies hit ground after traversing a horizontal distance of approximately 2500 m, as compared with a horizontal distance of 6500 m traversed by B^* if B moves independently of A; and this distance is only slightly sensitive to variations in such factors as the altitude of the separation zone, the cable length, and the location of attachment points $\bar{A}$ and $\bar{B}$, if kept within reason. The validity of this statement is investigated in the next section.

Results and Discussion

Figure 4 shows the paths traversed by B^* if the initial distances between $\bar{A}$ and $\bar{B}$ are 0.8 and 0.0 m, as when these points are located, relative to A^* and B^*, at $-2\boldsymbol{a}_1 + 0.4\boldsymbol{a}_3$ and

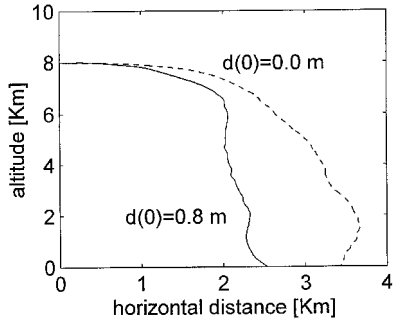

Fig. 4 Path traversed by B^* with different cable attachment points.

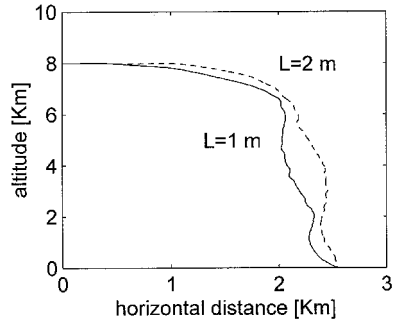

Fig. 5 Path traversed by B^* with different cable lengths.

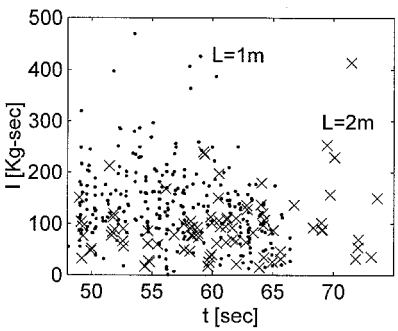

Fig. 6 Impulses experienced with different cable lengths.

$2\boldsymbol{b}_1 - 0.4\boldsymbol{b}_3$ m, and at $-2\boldsymbol{a}_1 + 0.4\boldsymbol{a}_3$ and $2\boldsymbol{b}_1 + 0.4\boldsymbol{b}_3$ m, respectively. These results indicate that shorter horizontal distances are obtained if $\bar{A}$ and $\bar{B}$ are initially located as far from one another as possible, so as to maximize the destabilizing effect of the first impacts.

Figure 5 shows the path traversed by B^* if the lengths of the cable are $L = 1$ m and $L = 2$ m, and indicates an insensitivity of the path to the length of the cable. Thus, Figs. 2, 4, and 5, and similar figures obtained for separation zones 2000–10,000 m high, indicate that the horizontal distance traversed by B^*, when B is connected to A with a cable, is 2500–3500 m, and that this distance depends primarily on the horizontal speed of B^* at the time of separation.

Figure 6 shows typical impulses exerted by $\bar{A}$ and $\bar{B}$ on one another through the cable when the cable becomes instantaneously taut. The dots stand for impulses associated with a 1-m-long cable, whereas the x signs indicate impulses occurring when the cable is 2 m long. One may conclude that the impulses do not exceed 500 kg-s. Moreover, the impulses are not sensitive to the length of the cable, nor are they sensitive to the location of $\bar{A}$ in A and of $\bar{B}$ in B, an observation supported by additional runs.

Lastly, the significance of the choice made for $\dot{d}_0$ is studied with the aid of Figs. 7 and 8. Figure 7 shows paths traversed by B^*, and Fig. 8 shows the associated tension in the cable, simulated with $\dot{d}_0 = 0.1$, 0.4, and 1.0 m/s. Figures 7 and 8

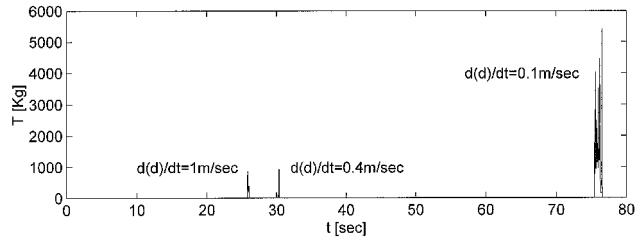

Fig. 7 Cable tension evaluated with different values of $\dot{d}_0$.

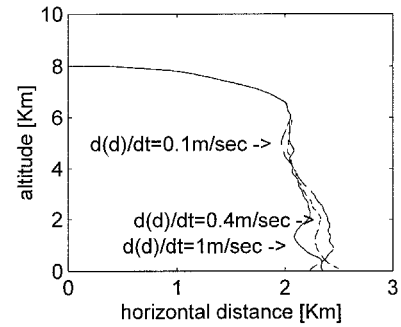

Fig. 8 Path traversed by B^* predicted with different values of $\dot{d}_0$.

indicate that, within limits, path (and impulse) predictions are not sensitive to the choice of $\dot{d}_0$, unlike tension predictions. However, based on a number of additional runs, one can estimate the peak value of the tension to be 6000 kg. Finally, one can show that, if $\dot{d}_0 < 0.015$ m/s, then the cable is considered loose throughout the simulation, and that this fact has a minor effect on the path traversed by B^*.

One can summarize the results as follows. The paths traversed by B^* can be predicted with reasonable accuracy, as are the associated impulses, whereas tension predictions depend on the choice of $\dot{d}_0$. A number of runs are required, with different $\dot{d}_0$, to establish an acceptable estimation of the tension peak value.

A final comment is in order. The model in Fig. 1 is a simple one, as implied by the various assumptions made in the sequel. It is nevertheless argued that, because the motion of the system is erratic, its main characteristics have been captured.

Conclusions

An algorithm has been presented that can be used to predict the motion of two cable-connected bodies in atmospheric free-fall. The path traversed by the bodies can be predicted with reasonable accuracy, as can the impulses associated with the impacts occurring when the cable becomes instantaneously taut or when the bodies collide with one another. The cable may become continuously taut, in which event it is possible to predict the associated tension. However, the tension predictions were found to be less conclusive. In general, higher tension levels tend to appear at a later part of the motion. Thus, if the cable is designed to withstand the impulses, it is likely to survive the crucial part of the motion. Thereafter, the missile parts move essentially downward. By that time, the main task of the cable is completed. The missile parts will hit the ground closer to one another and closer to the abortion zone. If no explosion takes place, minimum damage will be caused to the debris as compared with the damage caused by a mission terminated with an explosion.

References

[1]"Ariane Failure Report," *Aviation Week & Space Technology*, Sept. 9, 1996, pp. 79–81.

[2]Anselmo, J. C., "THAAD Fails Third Intercept," *Aviation Week & Space Technology*, July 22, 1996, p. 31.

[3]Liandong, L., and Bainum, P. M., "Effects of Tether Flexibility on the Tethered Shuttle Subsatellite Stability and Control," *Journal of Guidance, Control, and Dynamics*, Vol. 12, No. 6, 1989, pp. 866–873.

[4]Banerjee, A. K., and Kane, T. R., "Dynamics of Tethered Payloads with Deployment Rate Control," *Journal of Guidance, Control, and Dynamics*, Vol. 13, No. 4, 1990, pp. 759–762.

[5]Chocran, J. E., Innocenti, M., and Thurkal, A., "Dynamics and Control of Maneuverable Towed Flight Vehicle," *Journal of Guidance, Control, and Dynamics*, Vol. 15, No. 5, 1992, pp. 1245–1252.

[6]Guido, M., "Longitudinal Dynamics of a Towed Sailplane," *Journal of Guidance, Control, and Dynamics*, Vol. 16, No. 5, 1993, pp. 822–829.

[7]Frishwell, M. I., "Steady-State Analysis of Underwater Cables," *Journal of Waterway, Port, Coastal and Ocean Engineering*, Vol. 121, No. 2, 1995, pp. 98–104.

[8]Henderson, J. F., and Wright, R. C., "Underwater Terrain-Following Using Active Controls on a Towed Vehicle," *Underwater Technology*, Vol. 19, No. 3, 1993, pp. 14–22.

[9]Gao, C., and Hartsough, B. R., "Concepts for Harvesting Timber on Steep Terrain," *Transactions of the American Society of Agricultural Engineering*, Vol. 31, No. 2, 1988, pp. 362–368.

[10]Salsbery, B. P., and Hartsough, B. R., "Control of a Cable Towed Vehicle to Minimize Slip," *Journal of Terramechanics*, Vol. 30, No. 5, 1993, pp. 325–335.

[11]Peterson, U. N., Rukgauer, A., and Schiehlen, W. O., "Lateral Control of a Convoy Vehicle System," *Vehicle System Dynamics Supplement*, No. 25, 1996, pp. 519–532.

[12]Svestka, P., and Vleugels, J., "Exact Motion Planning for Tractor-Trailer Robots," *IEEE International Conference on Robotic and Automation Proceedings*, Vol. 3, Inst. of Electrical and Electronics Engineers, New York, 1995, pp. 2445–2450.

[13]Kane, T. R., and Levinson, D. A., *Dynamics, Theory and Applications*, McGraw–Hill, New York, 1985.